Carbohydrate Polymers 102 (2014) 584–589

Contents lists available at ScienceDirect

Carbohydrate Polymers

journal homepage: www.elsevier.com/locate/carbpol

Porous thin film barrier layers from 2,3-dicarboxylic acid cellulose nanofibrils for membrane structures

Miikka Visanko[a,*], Henrikki Liimatainen[b], Juho Antti Sirviö[c], Antti Haapala[b], Rafal Sliz[d], Jouko Niinimäki[b], Osmo Hormi[c]

[a] Fibre and Particle Engineering Laboratory & Thule Institute, University of Oulu, PO Box 4300, FI-90014 Oulu, Finland
[b] Fibre and Particle Engineering Laboratory, University of Oulu, PO Box 4300, FI-90014 Oulu, Finland
[c] Department of Chemistry, University of Oulu, PO Box 3000, FI-90014 Oulu, Finland
[d] Optoelectronics and Measurement Techniques Laboratory, University of Oulu, PO Box 4500, FI-90014 Oulu, Finland

ARTICLE INFO

Article history:
Received 24 September 2013
Received in revised form
27 November 2013
Accepted 3 December 2013
Available online 12 December 2013

Keywords:
Ultrafiltration
Cellulose nanofibrils
Rejection percentage
Periodate oxidation
Chlorite oxidation
Barrier layer

ABSTRACT

To fabricate a strong hydrophilic barrier layer for ultrafiltration (UF) membranes, 2,3-dicarboxylic acid cellulose nanofibrils with high anionic surface charge density (1.2 mekv/g at pH 7) and a width of 22 ± 4 nm were used. A simple vacuum filtration method combined with a solvent exchange procedure resulted in a porous layer with a thickness of ~0.85 μm. The fabricated membranes reached high rejection efficiencies (74–80%) when aqueous dextrans up to 35–45 kDa were filtrated to evaluate the molecular weight cut-offs (MWCO). A linear correlation between the barrier layer thickness and the flux rate was observed in all tested cases. Further optimization of the barrier layer thickness can lead to an even more effective structure.

1. Introduction

Continuing global population growth requires more efficient use of already meager fresh water resources. Consequently, advanced technological solutions are required so that future generations will not have to live under water scarcity (Kummu, Ward, Moel, & Varis, 2010). New innovations in membrane filtration technology offer potential for effective green solutions for the production of clean water without intensive chemical treatments (Shannon et al., 2008). For this purpose, high flux thin film coated ultrafiltration (UF) membranes can achieve the required features with notable impurity retention capabilities (Ma, Burger, Hsiao, & Chu, 2012). The sustainability of the thin film membrane can be further improved by replacing the present non-renewable polymeric materials from petrochemical resources with naturally occurring polymers like cellulose (Goetz, Mathew, Oksman, Gatenholm, & Ragauskas, 2009).

When cellulose fibers are processed to nano-size by chemical treatment (Liimatainen, Visanko, Sirviö, Hormi, & Niinimäki, 2012; Liimatainen, Visanko, Sirviö, Hormi, & Niinimäki, 2013b), enzymatic treatment (Henriksson, Henriksson, Berglund, & Lindström, 2007), mechanical treatment (Iwamoto, Nakagaito, & Yano, 2007), or a combination of these, individual nanofibrils or aggregates of them with widths from 3 nm to 4 nm (Saito, Kimura, Nishiyama, & Isogai, 2007) and 20–40 nm (Svagan, Azizi Samir, & Berglund, 2007), respectively, can be attained with lengths of several micrometers. Cellulose nanofibrils have the ability to form ultra-strong nanofibrous networks via hydrogen bonding (Henriksson, Berglund, Isaksson, Lindström, & Nishino, 2008). This feature makes nanocellulose an ideal candidate for membrane barrier layers, since it can withstand harsh conditions (e.g., high pressure and mechanical strain) without rupturing.

So far, cellulose nanofibrils have been used to fabricate self-standing, foldable, high-strength, and optically transparent nanopaper structures (Nogi, Iwamoto, Nakagaito, & Yano, 2009). The porosity of these tightly hydrogen-bonded nanopaper structures has been increased by applying a solvent exchange method (Henriksson et al., 2008), combined solvent exchange with

* Corresponding author. Tel.: +358456764533; fax: +35885532327.
E-mail addresses: miikka.visanko@oulu.fi (M. Visanko), Henrikki.Liimatainen@oulu.fi (H. Liimatainen), Juho.Sirvio@oulu.fi (J.A. Sirviö), Antti.Haapala@oulu.fi (A. Haapala), Rafal@ee.oulu.fi (R. Sliz), Jouko.Niinimaki@oulu.fi (J. Niinimäki), Osmo.Hormi@oulu.fi (O. Hormi).

0144-8617/$ – see front matter © 2013 Elsevier Ltd. All rights reserved.
http://dx.doi.org/10.1016/j.carbpol.2013.12.006

supercritical CO_2 drying (Sehaqui, Morimune, Nishino, & Berglund, 2012), liquid CO_2 evaporation, or tert-butanol freeze-drying (Sehaqui, Zhou, Ilkkala, & Berglund, 2011). Based on earlier studies, we hypothesize that these porous nanofibril structures could function as an effective membrane structure, as they have not yet been tested in membrane applications. Previously, biobased raw materials like chitosan (Yoon et al., 2006; Ma, Burger, Hsiao, & Chu, 2011) and cellulose nanofibrils (Ma et al., 2011) have only been used to cover an electrospun nanofibrous polyethylene terephthalate (PET) network in three-layer structures, but they have not been used as an active filtration network to form two-layer structures.

In this study, we fabricated a porous cellulose nanofibril layer on top of a commercial microfiltration (MF) membrane. A thin and porous nanostructured barrier layer was formed from 2,3-dicarboxylic acid cellulose (DCC) nanofibrils, which were obtained from sequential periodate-chlorite oxidation treatment (Liimatainen et al., 2012). The top barrier layer provides both the required selective separation of components in the sample and simultaneously acts as the protective support for the membrane. The bottom layer acts as a microporous fabrication platform, which supports and maintains the upper layer's form. The manufacture of the nanostructured top layer is based on a straightforward vacuum filtration method in which the residual water of the formed layer is solvent exchanged to ethanol to increase the membrane's porosity. The main objectives of the research were to study the potential of DCC-nanofibrils to form a functional barrier layer, and to examine its performance in a membrane filtration application. The membrane's functionality and structural characteristics were assessed by measuring pure water fluxes, molecular weight cut offs (MWCO), surface morphology, water contact angles, and mechanical properties. All the results were compared with two commercial cellulose-based membranes.

2. Experimental

2.1. Raw materials

Bleached birch (*Betula pendula*) chemical wood pulp was used as a raw material to produce cellulose nanofibrils for the top barrier layer of thin film composite (TFC) membranes. Pro analysis grade (p.a. grade) chemicals were purchased for oxidation pretreatment nanofibril preparation ($NaIO_4$, $NaClO_2$ and CH_3COOH) from Sigma-Aldrich (Germany) and were utilized without further purification. For polyelectrolyte titrations of nanofibrils, the following chemicals were used: 0.1/1 M NaOH and HCl, NaCl, NaCOO, $NaHCO_3$ (Merck, Germany), NaH_2PO_4 (Sigma-Aldrich, Germany), $NaCH_3COO$ (Oy FF Chemicals, Finland), Na_2HPO_4 (Fluka, Germany), and Na_2CO_3 (J.T. Baker, Germany), all of which were p.a. grade and were used as received. Poly(diallyldimethylammonium chloride) (poly-DADMAC, 20% aq.) used for titration was purchased from Sigma-Aldrich (Germany). The supporting hydrophilic bottom layer of the composite membrane (Durapore polyvinylidene fluoride (PVDF) 0.65 μm) was bought from Millipore (France). Dextrans (from *Leuconostoc mesenteroides*, Sigma-Aldrich, Germany) with molecular weights of 9–11 kDa, 35–45 kDa, 64–76 kDa, 150 kDa, and 2000 kDa were used for MWCO measurement. Cellulose-based reference membranes, UC030 and UC100, were kindly donated by Microdyn Nadir (Germany).

2.2. Preparation of 2,3-dicarboxylic acid cellulose (DCC) nanofibrils

The cellulose nanofibrils were prepared using a combination of oxidative chemical pretreatment and mechanical homogenization. As a pretreatment, sequential sodium metaperiodate and sodium chlorite oxidation was used for the bleached chemical wood pulp to produce 2,3-dicarboxylic acid cellulose according to a previously reported method (Liimatainen et al., 2012). In brief, the pulp was first oxidized with the sodium metaperiodate oxidation for three hours to obtain dialdehyde cellulose fibers (Sirviö, Hyväkkö, Liimatainen, Niinimäki, & Hormi, 2011), after which the aldehydes were converted to carboxylic acid groups using sodium chlorite oxidation for 48 h. Oxidized cellulose fibers were converted to nanofibrils using a two-chamber high-pressure homogenizer (APV-2000, Denmark). Two passes, with pressures of 650 bar and 900 bar, respectively, were enough to produce a clear viscous DCC-nanofibril gel.

2.3. Preparation of pH buffers and determination of apparent charge density of DCC-nanofibrils

The pH buffer solutions were fabricated by diluting an appropriate amount of Na-salt of the respective base to approximately 80% of the final volume, adjusting the pH (as measured by a combination of electrode, (Mettler Toledo)) with 0.1/1 M of HCl or NaOH, and, finally, diluting the buffer to the appropriate volume in a volumetric flask. The buffer solutions used in the analysis were all in the pH range of 3–10 and, thus, both the buffer concentration and ionic strength (as $[Na^+]$) were kept constant. The pH 10 solution was prepared using Na_2CO_3 as the base, and in this sample the ionic strength was higher. The polyelectrolyte titrations were conducted with a Mütek PCD-Two particle charge detector (Germany) by adding aqueous poly-DADMAC (1.0 mekv dm^{-3}) to the anionic DCC-nanofibril solution while monitoring the signs of the solution charge.

2.4. Preparation of nanofibrous cellulose thin film composite membrane

Two layer membrane structures with top DCC-nanofibril barrier layers were prepared on the commercial support layer, and three different top layer thicknesses were tested. First, the homogenized nanofibril suspension was diluted to 0.3% concentration by mixing with deionized water using the UltraTurrax mixer (IKA T25, Germany) at 10,000 rpm for 3 min. After the dilution, the suspension was vacuum filtrated in a glass filter funnel (7.2 cm in diameter) using a filter membrane (pore size 0.65 μm) at the bottom. The overall filtration time was less than 10 min, depending on the amount of nanofibrils used. After filtration, a wet thin film was formed on top of the bottom layer. The remaining water from the wet layer was solvent exchanged to ethanol (96%) by placing the sample in an ethanol bath overnight. Solvent exchanged samples were dried in a desiccator until all of the remaining ethanol was evaporated. The wet strength of the barrier layer was improved by placing the dried sample in a 10% $CaCl_2$ solution. This treatment was carried out for 30 min, followed by washing with deionized water to abolish the remaining $CaCl_2$. The $CaCl_2$ treatment is assumed to crosslink carboxylic acid groups via Ca^{2+} ions, which enhance the strength of the contact points. All the manufactured membranes were tested immediately without storage.

2.5. Field-emission scanning electron microscopy (FESEM)

Images of the freeze-dried and sputter-coated (Pd) samples were taken with an FESEM (Zeiss ULTRA plus, Germany) at an accelerating voltage of 5 kV. Three different types of samples were imaged: individual nanofibrils filtered on top of a 0.2 μm membrane (Nuclepore, Whatman, United Kingdom), surface morphology of the DCC-nanofibril barrier layer, and

cross-sectioned membrane samples fractured using liquid nitrogen freezing.

2.6. FT-IR spectroscopy

The crosslinking between Ca^{2+} ions and carboxylic acid groups was studied with FT-IR spectroscopy. Two membrane samples were made for the analysis, where the crosslinked sample was fabricated according the procedure described in chapter 2.4. A non-crosslinked sample was made directly to water without $CaCl_2$ treatment. Both the samples were freeze dried and after drying the barrier layers were carefully peeled off from the bottom layer and pressed into KBr pellets. Transmission mode FT-IR spectra were collected with Bruker FT-IR spectrometer (USA). Spectra were obtained in 400–4000 cm^{-1} range and for each sample 32 scans were taken at a resolution of 4 cm^{-1}.

2.7. Molecular weight cut-off (MWCO)

A series of dextrans with different molecular weights were used to test the MWCO of the DCC-nanofibril based composite membrane and commercial reference membranes. Feed solutions of 1000 ppm were produced by dissolving dextrans in Milli-Q water under vigorous stirring with a magnetic stirrer. All the membranes were pre-wetted with Milli-Q water for 10 min prior to testing. A stirred UF cell (Millipore, model 8050, France) was applied for the filtration of feed solutions. To equilibrate the membrane and open clogged pores, Milli-Q water was filtered for 30 min at a pressure of 1 bar in the case of the DCC-nanofibril based membranes. The reference membranes (UC030 and UC100) were equilibrated by filtrating 50 ml of Milli-Q water at 1 bar.

For the MWCO test, 50 ml of dextran feed solution was added to the stirred UF cell at room temperature. First, 5 ml of the permeate was discarded and the next 5 ml was collected for the total organic carbon analyzer (TOC, Sievers 900, USA). From the collected permeate, a dilution to <20 ppm was made. The TOC measurement was repeated twice for each data point. By using the averaged results from the TOC analysis, the rejection percentage ($R\%$) was calculated according to the following equation:

$$R\% = \frac{C_f - C_p}{C_f} \times 100\% \quad (1)$$

where C_f and C_p are the feed and permeate concentrations of the solutions, respectively.

2.8. Pure water flux

To test the membranes' performance, pure water flux measurements were obtained using a stirred UF dead-end cell (Millipore, model 8050, France) at 700 rpm at room temperature. Measurements were carried out by pressurizing a dispensing pressure vessel with nitrogen. Permeate from the dead-end cell was collected and weighted on an analytical balance. Three measurements were performed at pressures of 1–3 bar. All the membranes were pre-wetted in deionized water prior to use.

2.9. Water contact angle measurement

The hydrophilicity of the DCC-nanofibril based membranes and commercial reference membranes (UC030 and UC100) were investigated by applying a static sessile-drop contact-angle measurement method. Milli-Q water was used as a probe liquid at room temperature with a Krüss DSA100 (Germany) system. The instrument was equipped with a high speed camera (360 fps) and analysis software. The contact angle was determined immediately after the formation of the drop on the film surface. Contact angles were extracted by the height-width method, where a rectangle enclosed by contour line is regarded as being the segment of a circle. As a result, contact angles could be calculated from the height-width relationship of the enclosing rectangle. For each sample, three droplets on different locations were studied, the results were averaged, and standard deviations were calculated.

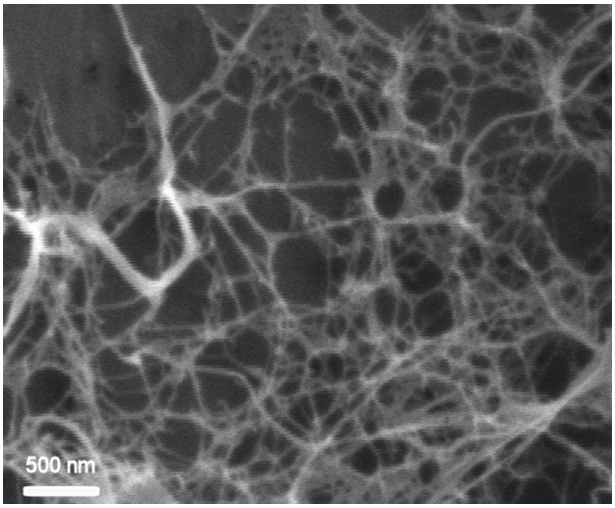

Fig. 1. FESEM image of individual DCC-nanofibrils after two passes through a high-pressure homogenizer.

3. Results and discussion

3.1. Characterization of DCC-nanofibrils

According to the FESEM image shown in Fig. 1, DCC-nanofibrils with an average width of 22 ± 4 nm and a length of several micrometers were produced. The average widths were calculated by measuring several different individual nanofibrils from the image data using a digital slide caliper. However, the freeze-drying sequence of the sample preparation is assumed to cause nanofibril aggregation, so it is likely the widths of independent nanofibrils were actually thinner. A study in which nanofibrils were imaged with atomic force microscopy (AFM) in aqueous and dried states indicated a clear difference between the sample preparation methods: the dried samples had an average width of more than double that of the never dried samples (Olszewska et al., 2011). Furthermore, our previous AFM analysis of similarly manufactured DCC-nanofibrils indicated that the nanofibrils had a typical width of 3–5 nm (Liimatainen et al., 2013a).

3.2. Apparent charge density of DCC-nanofibrils

As previously shown (Liimatainen et al., 2012), DCC-nanofibrils fabricated with the same oxidation sequence can reach high carboxyl content (1.75 mmol g^{-1}). This should be beneficial for the performance of the membrane, as the high anionic surface charge increases repulsion towards anionically charged colloidal material, and this effect, in turn, reduces the fouling of the membrane. Thus, changes in the charge density of DCC-nanofibrils can be assumed to affect the performance of the membrane. Consequently, the influence of pH on the charge behavior of DCC-nanofibrils was studied. According to Fig. 2, alkaline conditions did not affect the charge density of DCC-nanofibrils, which started to decrease in acidic conditions at pH below 5. Dramatic decrease was observed when the pH was lowered to 3, which is below the pK_a values of both dicarboxyl acid groups of DCC-nanofibrils (Kim & Kuga, 2001). High surface charge reduces the fouling of the DCC-nanofibril based

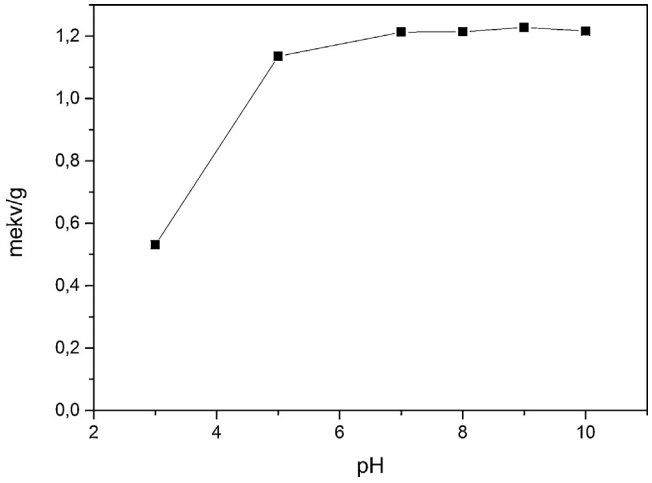

Fig. 2. Apparent anionic charge density of DCC-nanofibrils as a function of pH.

membranes and, hence, it is likely their long term performance will be optimal in conditions where the filtrate has a pH of 5 or higher.

3.3. Fabrication of DCC-nanofibril based composite membranes

A two-layered membrane based on a DCC-nanofibril barrier layer and a commercial (MF) support layer (pore size 0.65 μm) was manufactured by vacuum filtration and solvent exchange procedures. The main ambition of the study was to investigate the potential of DCC-nanofibrils to function as a protective cellulose barrier layer in UF membranes. Millipore's 0.65 μm membrane was selected as the supporting bottom layer due to its consistent behavior in preliminary investigations. Other platforms have been also tested and there is an ongoing investigation to replace the bottom layer with more open and microporous structures for better functionality.

Porosity of the protective DCC-nanofibril barrier layer was propagated after the vacuum filtration by exchanging the remaining water from the moist gel cake to ethanol. The usage of a less polar liquid such as ethanol mitigates the strong hydrogen bonding nature of the nanofibrils and enables the formation of a more porous nanofibril network in which the interfibril bonds become weakened (Henriksson et al., 2008). Higher porosity that maintains the same pore size distribution leads to more expedient fluxes and better economic viability. Moreover, it is of great interest to produce porous barrier layers without greatly compromising their mechanical properties.

3.4. Surface morphology and structure characterization

The structure of DCC-nanofibril based membranes was further analyzed by imaging surface layer and cross-sectional views of the samples with FESEM. In Fig. 3(a), the porous structure of the DCC-barrier layer that formed as a result of the solvent-exchange treatment can be seen. The pore size of the barrier layer is not uniform and the pore sizes estimated from Fig. 3(a) range from roughly 17 nm to 51 nm. The pore size of the barrier layer is discussed in detail in chapter 3.6.

The thicknesses of the barrier layers were estimated from the cross-sectional images (Fig. 3(b)). The thicknesses were 3.35 μm, 1.65 μm, and 0.85 μm, and the initial mass fractions between samples were 100/75/50%, respectively. Barrier layer thickness was doubled when the mass fraction of the added nanofibrils was increased by 25%. Fabrication of the DCC-nanofibril barrier layer with vacuum filtration on top of the Durapore PVDF membrane

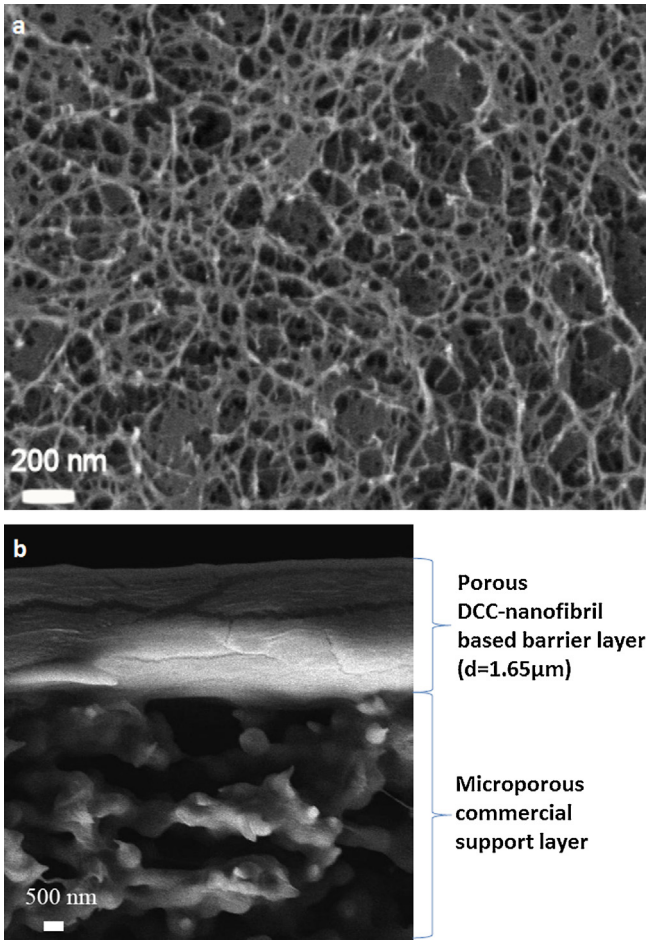

Fig. 3. (a) Surface and (b) cross-sectional images of the fabricated DCC-nanofibril membranes with a barrier layer thickness of ~1.65 μm.

(0.65 μm) affected the final thickness of the protective layer. A barrier layer of 0.85 μm thickness was the minimum that could be reached without losing surface uniformity. Use of fewer nanofibrils resulted in visible defects on the surface of the barrier layer. The supporting bottom layer had a thickness of 125 μm.

3.5. FT-IR spectroscopy

FT-IR spectrum of non-crosslinked membrane showed characteristic band due to the C=O stretch of deprotonated carboxylic acid at 1616 cm^{-1}(Fig. 4). After calcium crosslinking, this band shifted to higher wavenumber (1621 cm^{-1}). This is probable due to the different interaction between monovalent sodium and divalent calcium ions with carboxylic acid groups of DCC. This indicates the formation of crosslinked structure between calcium and DCC.

3.6. Molecular weight cut-offs (MWCO) of membranes

To evaluate the pore size and rejection performance of both the DCC-nanofibril barrier layer and the commercial cellulose based membranes, MWCO measurements were taken using a series of aqueous dextrans with various molecular weights. The DCC-nanofibril barrier layer reached MWCO values above 90% when a 2000 kDa dextran solution was used with the two thickest barrier layers. The thinnest barrier layer had a lower MWCO with the 2000 kDa dextran (74%), and we think this might be caused by the larger defects on the surface of the thinner layer. The whole dextran series was performed for the two structures with the most

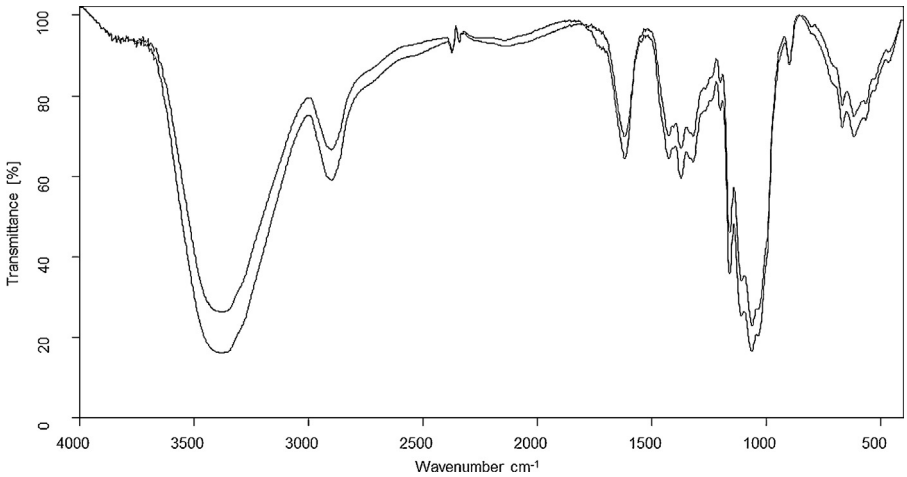

Fig. 4. FT-IR spectra for $CaCl_2$ treated barrier layer (upper) and non-crosslinked sample (lower).

potential, those with barrier layer thicknesses of 0.85 μm and 1.65 μm, shown in Fig. 5. An operating pressure of 1 bar was selected to reduce the compression of the barrier layer. The DCC-nanofibril barrier layer has an interconnected nanofibril network with tortuous random pores instead of straight-through pores, and the tortuosity (τ) was expected to be high. The high rejection percentages may be a consequence of the network structure where the dextrans are captured in the interior of the membrane (dead-end pores) during the filtration test.

Compared to the commercial reference membranes, the structure of the DCC-nanofibril barrier layers seems to be tighter, as greater rejection percentages were achieved. The DCC-nanofibril barrier layers held a high rejection percentage of around 74–80% up to 35–45 kDa dextran solutions, which was twice as high as the most effective reference membrane (UC030). A clear decrease was observed only with the smallest molecular weight dextran solutions (9–11 kDa). The manufacturer of the commercial cellulose based membranes reports a rejection percentage of 97–99% for UC100 with 2000 kDa dextran. Reference membrane UC030 has a reported rejection rate of 76–93% for Polyvinylpyrrolidone K 30 (average molecular weight of 40 kDa). The manufacturer's testing

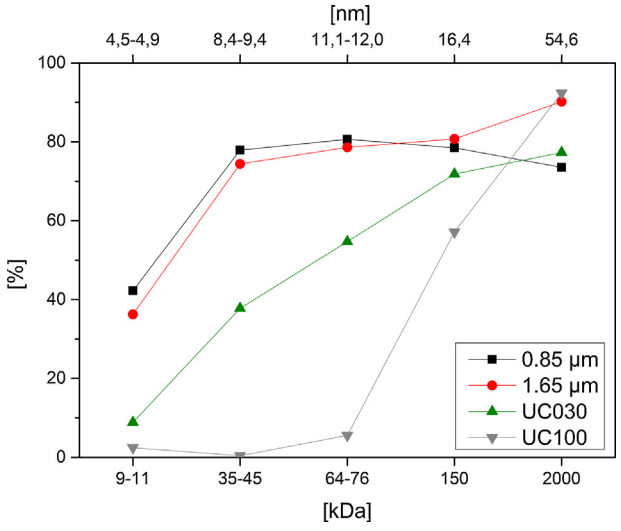

Fig. 5. Rejection percentage of dextrans with different molecular weights and corresponding particle diameter of dextrans for DCC-nanofibril membranes and commercial references.

conditions were 3 bar at 20 °C, with a stirred cell set to revolve at 700 rpm.

The MWCO test values are even higher than for previously reported thin film nanofibrous composite (TFNC) membrane materials (Ma et al., 2011) where the barrier layer was fabricated from ultrafine TEMPO-oxidized cellulose nanofibrils. The TEMPO-nanofibril barrier layer held a high rejection percentage (~80%) only up to 425–575 kDa dextrans, after which the rejection rate dropped significantly to ~30% with a 100–150 kDa dextran solution. The reason for this behavior may be the very thin layer thickness of TEMPO materials.

3.7. Pure water flux and water contact angle

To evaluate the filtration capacity of DCC-nanofibril membranes, pure water fluxes were measured with different barrier layer thicknesses. Operating pressure was adjusted to 1–3 bar in increments of 1 bar. Results from 30 min of filtration tests are presented in Fig. 6 for both DCC-nanofibril (a) and commercial reference membranes (b). The thickness of the DCC-nanofibril membrane barrier layers clearly correlated with D'Arcy's law (2), which states how profusely the flux depends on the barrier layer thickness:

$$J = \frac{K \times P}{\eta \times L}, \tag{2}$$

where J is the flux, K is the hydraulic permeability of the membrane, P is the pressure, η is the viscosity of the liquid, and L is the thickness of the membrane. Results presented in the Fig. 6a show clearly that the flux increases to about double when the layer thickness decreases from 1.65 μm to 0.85 μm. The same trend can be seen when the two thickest barrier layers are compared. If an even thinner layer was to be fabricated by casting, for example, and the trend continued, a ~0.20 μm barrier layer thickness would attain flux values of around 570 kg m^{-2} h^{-1} bar^{-1} with 3 bar of pressure, assuming the mechanical integrity of the thinner film would still withstand the strain.

According to the MWCO test results (Section 3.6), the DCC-nanofibril membranes clearly held a higher rejection percentage than the commercial reference membranes. This indicates that the DCC-nanofibril membranes had a smaller pore size and the pore size distribution was narrower, which partly explains the lower water flux values. The commercial reference membranes had a slightly higher affinity to water, as the water contact angles were $35.8 \pm 6.9°$ and $27.4 \pm 12.0°$ for UC030 and UC100, respectively. The heterogeneous surface structure of the reference

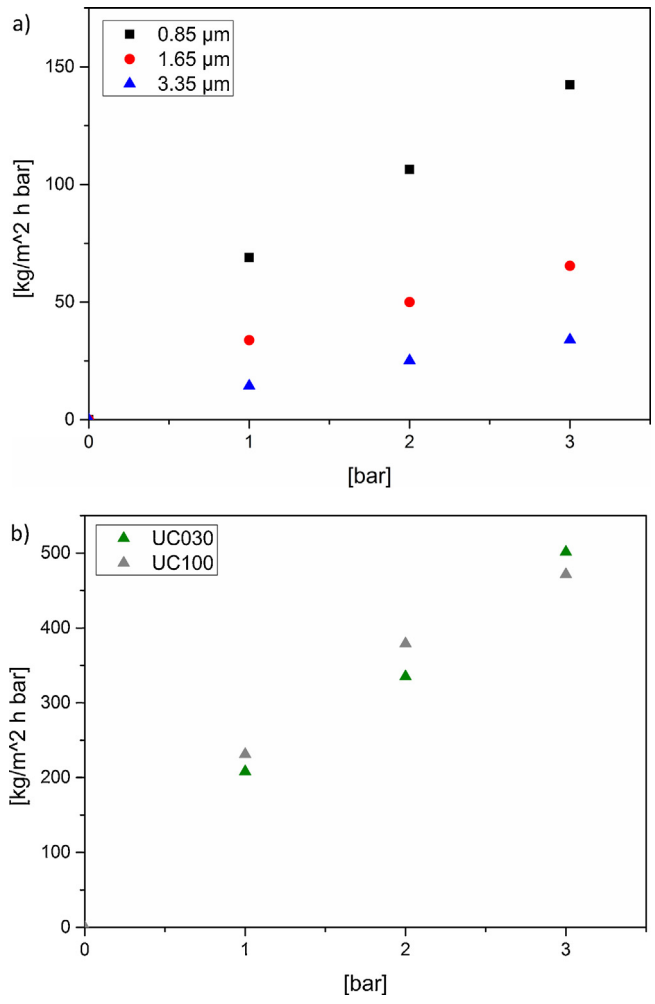

Fig. 6. Pure water fluxes for (a) DCC-nanofibril based membranes with different barrier layer thicknesses and (b) commercial reference membranes.

membranes is suspected to cause the deviation in the results as the measurement was repeated 3 times and up to 12 locations of the samples were analyzed. The DCC-nanofibril membranes had an average water contact angle of $45.0 \pm 4.7^{\circ}$, which are very similar to the contact angles in self-standing TEMPO-oxidized cellulose nanofibrils (Rodionova, Eriksen, & Gregersen, 2012). The DCC-nanofibril barrier layer was still clearly hydrophilic, as the sodium chlorite oxidation created hydrophilic, highly anionically charged carboxylic acid groups on the surface of cellulose nanofibrils.

4. Conclusions

Sequential sodium metaperiodate and sodium chlorite oxidized cellulose nanofibrils with high surface charge showed great potential to function as a barrier layer for UF applications. According to the MWCO tests, the manufactured barrier layers had an ideal pore size for UF applications, as the rejection percentages remained high (74–80%) when tested with up to 35–45 kDa dextran solution. The pore size distribution was uneven, influenced by both the DCC-nanofibrils' irregular nanofibril diameter and the random structure of the nanofibril network. Permeation flux values correlated decidedly with the barrier layer thickness, and to further improve the effectiveness of the membrane, fabrication of a thinner DCC-nanofibril layer is under investigation. Overall, the DCC-nanofibrils showed promising results as an environmentally friendly alternative for UF membrane barrier layers.

Acknowledgements

This work was carried out as part of the Future Biorefinery Program of Finnish Bioeconomy Cluster. Financial support from the Thule Institute is acknowledged.

References

Goetz, L., Mathew, A., Oksman, K., Gatenholm, P., & Ragauskas, A. J. (2009). A novel nanocomposite film prepared from crosslinked cellulosic whiskers. *Carbohydrate Polymers*, 85–89.

Henriksson, M., Henriksson, G., Berglund, L. A., & Lindström, T. (2007). An environmentally friendly method for enzyme-assisted preparation of microfibrillated cellulose (MFC) nanofibers. *European Polymer Journal*, 3434–3441.

Henriksson, M., Berglund, L. A., Isaksson, P., Lindstrom, T., & Nishino, T. (2008). Cellulose nanopaper structures of high toughness. *Biomacromolecules*, 1579–1585.

Iwamoto, S., Nakagaito, A. N., & Yano, H. (2007). Nano-fibrillation of pulp fibers for the processing of transparent nanocomposites. *Applied Physics A*, 461–466.

Kim, U. J., & Kuga, S. (2001). Ion-exchange chromatography by dicarboxyl cellulose gel. *Journal of Chromatography A*, 29–37.

Kummu, M., Ward, P. J., Moel, H., & Varis, O. (2010). Is physical water scarcity a new phenomenon? Global assessment of water shortage over the last two millennia. *Environmental Research Letters*, 1–10.

Liimatainen, H., Visanko, M., Sirviö, J., Hormi, O., & Niinimäki, J. (2012). Enhancement of the nanofibrillation of wood cellulose through sequential periodate-chlorite oxidation. *Biomacromolecules*, 1592–1597.

Liimatainen, H., Sirviö, J., Visanko, M., Suopajärvi, T., Ezekiel, N., Hormi, O., & Niinimäki, J. (2013). Nanomaterials nanofibrillation of cellulose pulp using regioselective periodate pre- treatments. In M. T. Postek, R. J. Moon, A. W. Rudie, & M. A. Bilodeau (Eds.), *Production and Applications of Cellulose* (pp. 183–184). U.S.A: Tappi Press.

Liimatainen, H., Visanko, M., Sirviö, J., Hormi, O., & Niinimäki, J. (2013). Sulfonated cellulose nanofibrils obtained from wood pulp through regioselective oxidative bisulfite pre-treatment. *Cellulose*, 741–749.

Ma, H., Burger, C., Hsiao, B. S., & Chu, B. (2011). Ultrafine polysaccharide nanofibrous membranes for water purification. *Biomacromolecules*, 970–976.

Ma, H., Burger, C., Hsiao, B. S., & Chu, B. (2012). Highly permeable polymer membranes containing directed channels for water purification. *ACS Macro Letters*, 723–726.

Nogi, M., Iwamoto, S., Nakagaito, A. N., & Yano, H. (2009). Optically transparent nanofiber paper. *Advanced Materials*, 1595–1598.

Olszewska, A., Eronen, P., Johansson, L.-S., Malho, J.-M., Ankerfors, M., Lindstrom, T., Ruokolainen, J., Laine, J., & Österberg, M. (2011). The behaviour of cationic nanofibrillar cellulose in aqueous media. *Cellulose*, 1213–1226.

Rodionova, G., Eriksen, Ø., & Gregersen, Ø. (2012). TEMPO-oxidized cellulose nanofiber films: Effect of surface morphology on water resistance. *Cellulose*, 1115–1123.

Saito, T., Kimura, S., Nishiyama, Y., & Isogai, A. (2007). Cellulose nanofibers prepared by TEMPO-mediated oxidation of native cellulose. *Biomacromolecules*, 2485–2491.

Sehaqui, H., Zhou, Q., Ilkkala, O., & Berglund, L. A. (2011). Strong and though cellulose nanopaper with high specific surface area and porosity. *Biomacromolecules*, 3638–3644.

Sehaqui, H., Morimune, S., Nishino, T., & Berglund, L. A. (2012). Stretchable and strong cellulose nanopaper structures based on polymer-coated nanofiber networks: An alternative to nonwoven porous membranes from electrospinning. *Biomacromolecules*, 3661–3667.

Shannon, M. A., Bohn, P. W., Elimelech, M., Georgiadis, J. G., Mariñas, B. J., & Mayes, A. M. (2008). Science and technology for water purification in the coming decades. *Nature*, 301–310.

Sirviö, J., Hyväkkö, U., Liimatainen, H., Niinimäki, J., & Hormi, O. (2011). Periodate oxidation of cellulose at elevated temperatures using metal salts as cellulose activators. *Carbohydrate Polymers*, 1293–1297.

Svagan, A. J., Azizi Samir, M. A. S., & Berglund, L. A. (2007). Biomimetic polysaccharide nanocomposites of high cellulose content and high toughness. *Biomacromolecules*, 2556–2563.

Yoon, K., Kim, K., Wang, X., Fang, D., Hsiao, B. S., & Chu, B. (2006). High flux ultrafiltration membranes based on electrospun nanofibrous PAN scaffolds and chitosan coating. *Polymer*, 2434–2441.